

**Synthesis and Structural Properties of**  
***N*-(2-bromo-4-nitrophenyl)-3-methoxy-4-oxo-3,4-dihydro-2*H*-benzo[e][1,2]thiazine-3-carboxamide 1,1-dioxide:**  
**A Comparative Experimental and Quantum Chemical Study**

<sup>1,2</sup>Muhammad Nadeem Arshad, <sup>3</sup>Naveen Kosar, <sup>1,2</sup>Adullah Muhammad Asiri, <sup>3</sup>Khurshid Ayub  
<sup>4</sup>Islam Ullah Khan and <sup>3</sup>Tariq Mahmood\*

<sup>1</sup>Chemistry Department, Faculty of Science, King Abdulaziz University, P. O. Box 80203,  
Jeddah 21589, Saudi Arabia.

<sup>2</sup>Centre of Excellence for Advanced Materials Research (CEAMR), King Abdulaziz University,  
P. O. Box 80203, Jeddah 21589, Saudi Arabia.

<sup>3</sup>Department of Chemistry, COMSATS Institute of Information Technology, Abbottabad, Pakistan.

<sup>4</sup>Materials Chemistry Laboratory, Department of Chemistry, GC University, Lahore 54000, Pakistan.  
mahmood@ciit.net.pk\*

(Received on 3<sup>rd</sup> August 2016, accepted in revised form 23<sup>rd</sup> May 2017)

**Summary:** *N*-(2-bromo-4-nitrophenyl)-3-methoxy-4-oxo-3,4-dihydro-2*H*-benzo[e][1,2]thiazine-3-carboxamide-1,1-dioxide was synthesized in three step process with 86 % overall yield. The final structure of compound was evaluated by using spectroscopical methods (<sup>1</sup>H-NMR and FT-IR). Suitable crystals were obtained by slow evaporation method, and the final structure was confirmed unequivocally by performing single crystal X-ray diffraction (XRD) studies. Geometric parameters were calculated at B3LYP/6-31G (d, p) method with the help of Gaussian 09 software to validate spectroscopic and single crystal X-ray results. The computed data corroborated nicely with the experimental results (spectroscopic and X-ray). Frontier molecular orbitals (FMOs) and reactivity indices revealed the reactivity of benzothiazine derivative. Molecular electrostatic potential (MEP) was measured to understand the electro or nucleophilic nature of compound. Mulliken and natural population charge analysis (NBO) was carried out to prove inter and intramolecular hydrogen bonding.

Keywords: (a) 1,2-benzothiazine; (b) XRD; (c) Density Functional Theory (DFT); (d) FMOs; (e) MEP.

## Introduction

Benzothiazines, a class of heterocyclic compounds, are very well known for their broad range of pharmaceutical applications [1]. Various compounds belonging to the benzothiazine family are commercially available as anti-inflammatory drugs including piroxicam, meloxicam, cinnoxamic and droxicam etc. [2]. Benzothiazines have been extensively evaluated for their antibacterial [3], antifungal [4], antioxidant [5], anticonvulsant [6], anticancer [7] activities.

1,2-Benzothiazine-1,1-dioxide and their derivatives were nicely synthesized by using sodium saccharin as a cheaper raw material [8]. And first of all, Lombardino and co-workers discover anti-inflammatory activity of 1,2-benzothiazine having 3-carboxamide functionality [9]. Since then a number of different ways have been explored to synthesize various derivatives of carboxamides of 1,2-benzothiazines [10-12]. These synthetic methods include ring expansion multi-step synthesis [13], one pot strategy [14] and metal catalyzed Heck or Suzuki coupling reactions [15]. Ionic liquids were also employed to synthesize a series of *N*-alkylated derivatives of benzothiazine carboxamides [16]. 7-{3-[4-(2-Quinolinylmethyl)-1-piperazinyl]propoxy}-2,3-dihydro-4*H*-benzothiazin-3-one was proved as

selective potent anti-histamine agent when it was administer to Guinea pig [17]. Some benzothiazines derivatives were proved as good reducers [18] of cholesterol level by inhibiting the synthesis of cholesterol molecules. Sudoxicam was tested in vivo on rabbit and dogs, and shown as better anti-coagulant than aspirin [19]. Another study was designed with the aim to investigate and compare the actions of two NSAIDs i.e. Meloxicam (COX-2 inhibitor) and piroxicam (COX-1 inhibitor) for oxyradical production in rat gastric mucosa, and observed that both the oxicams showed gastric mucosal damage at similar extent [20].

Computational based methods have proven their importance to validate the different aspects of experimental results, but also to explore and investigate the detailed structural properties. Density functional theory (DFT) calculation is famous method to investigate the structure property relationship [21]. In continuation to our previous work regarding the synthesis and structural investigations on various benzothiazine and heterocyclic derivatives [22-28], the synthesis, XRD and density functional theory studies of benzothiazine derivative *N*-(2-bromo-4-nitrophenyl)-3-methoxy-4-oxo-3,4-dihydro-2*H*-benzo[e][1,2]thiazine-3-carboxamide 1,1-dioxide has been reported for the first time.

---

\*To whom all correspondence should be addressed.

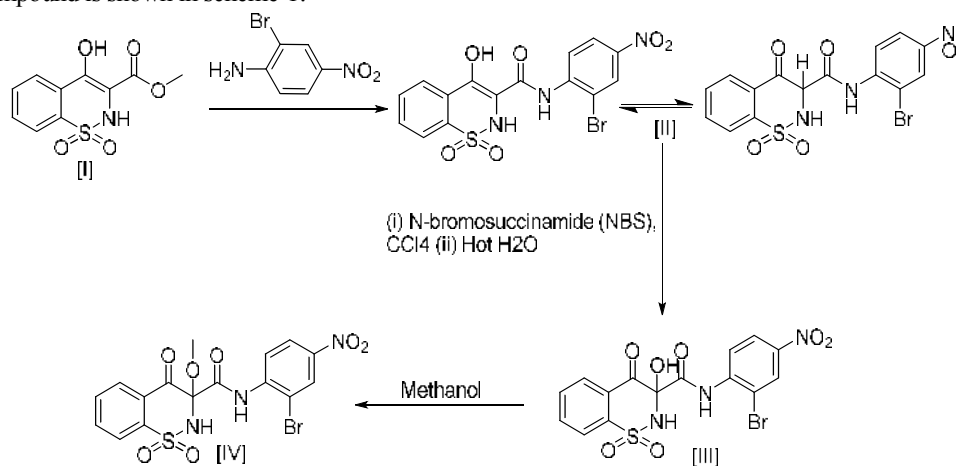
## Experimental

### Material and Methods

The chemicals used in synthesis were purchased from E. Merck, Sigma Aldrich and Alfa-Aesar and used without further purification. GF<sub>254</sub> aluminum based TLC plates purchased from MERK used to monitor the reaction progress. Varian AM400 instrument was used to record <sup>1</sup>H-NMR spectrum and chemical shifts are reported in ppm by considering tetramethylsilane as internal standard. FT-IR spectrum recorded on a Perkin Elmer 1600-FT spectrometer. Electrothermal (Griffin 1090) was used to measure the melting point and is reported as uncorrected.

### Synthesis of *N*-(2-bromo-4-nitrophenyl)-3-methoxy-4-oxo-3,4-dihydro-2*H*-benzo[*e*][1,2]thiazine-3-carboxamide 1,1-dioxide

4-Hydroxy-1,1-dioxo-1,2-dihydro-1λ<sup>6</sup>-benzo[*e*][1,2]thiazine-3-carboxylic acid methyl ester (0.25 g, 0.98 mmol) (**I**) was refluxed with 2-bromo-4-nitro-phenylamine (0.211 g, 0.98 mmol) in xylene as solvent to yield 4-hydroxy-1,1-dioxo-1,2-dihydro-1λ<sup>6</sup>-benzo[*e*][1,2]thiazine-3-carboxylic acid (2-bromo-4-nitro-phenyl)amide (**II**). The precipitate obtained were treated with *N*-bromosuccinamide (0.171 g, 0.98 mmol) in the presence of benzoyl peroxide as catalyst and carbon tetrachloride (CCl<sub>4</sub>) as solvent followed by washing with hot water to obtain *N*-(2-bromo-4-nitrophenyl)-3-hydroxy-4-oxo-3,4-dihydro-2*H*-benzo[*e*][1,2]thiazine-3-carboxamide-1,1-dioxide (**III**). Then the compound molecule (**III**) was crystallized in methanol, where dehydration occur between two alcohols during recrystallization to furnish *N*-(2-bromo-4-nitrophenyl)-3-methoxy-4-oxo-3,4-dihydro-2*H*-benzo[*e*][1,2]thiazine-3-carboxamide 1,1-dioxide (**IV**). The detailed synthesis of the title compound is shown in scheme-1.



Scheme-1: Synthetic scheme of title compound *N*-(2-bromo-4-nitrophenyl)-3-methoxy-4-oxo-3,4-dihydro-2*H*-benzo[*e*][1,2]thiazine-3-carboxamide 1,1-dioxide (**IV**).

State: white powder, Yield: 86%, M. P. 144-146°C, FT-IR (KBr)  $\nu_{\max}$ : 3350, 1750, 1699, 1322, 1176  $\text{cm}^{-1}$  <sup>1</sup>H-NMR: (400 MHz) (CDCl<sub>3</sub>)  $\delta$ : 8.55 (1H, s, CONH), 7.64-8.42 (7H, m, aromatic), 3.68 (1H, s, OCH<sub>3</sub>)

*Crystal data*: C<sub>16</sub>H<sub>12</sub>N<sub>3</sub>O<sub>7</sub>SBr,  $M_r = 470.26$   $\text{g}\cdot\text{mol}^{-1}$ , colorless block, 0.36mm × 0.31mm × 0.25mm, orthorhombic, space group *Pbca*,  $a = 20.813(1)$ ,  $b = 13.187(7)$ ,  $c = 13.062(8)$  Å,  $\alpha = \beta = \gamma = 90^\circ$ ,  $V = 3584.8(3)$  Å<sup>3</sup>,  $Z = 8$ ,  $D_c = 1.743$   $\text{g}\cdot\text{cm}^{-3}$ ,  $F(000) = 1888$ , MoK $\alpha$  radiation,  $\lambda = 0.71073$  Å,  $T = 296(2)$  K,  $2\theta_{\max} = 56.61^\circ$ , 18515 reflections collected, 4348 unique ( $R_{\text{int}} = 0.099$ ), final  $GOOF = 0.923$ ,  $R = 0.053$ ,  $wR = 0.0784$ ,  $R$  indices based on 1643 reflections with  $I > 2\sigma(I)$  (refinement on  $F^2$ ) 254 parameters,  $\mu = 2.457$   $\text{mm}^{-1}$ .

### Crystallography

Suitable crystal was chosen under microscope and pasted on glass tip with the help of glue, and displayed on Bruker KAPPA APEX II diffractometer [29], having Mo-K $\alpha$  radiation source. The crystal structure was solved with the help of SHELXS-97 [30] and refinements were resolved by full-matrix least-squares approach on  $F^2$  using SHELXL-97 [30]. C, N, O and S were refined with the help of anisotropic parameters. Aromatic hydrogens were positioned geometrically (C-H<sub>arom.</sub> = 0.93 Å), and treated with the help of riding model having  $U = 1.2$  times for aromatic carbons. The hydrogens for methyl group were also refined geometrically and treated with riding model having C-H = 0.97 Å and  $U = 1.5$  times for methyl carbon atom. Both the (N-H = 0.86 Å) hydrogen atoms were also refined at calculated positions with  $U = 1.2$  for nitrogen atom. ORTEP-III [31] and PLATON [32] inbuilt within the WINGX [33, 34] were used to draw the molecular diagrams.

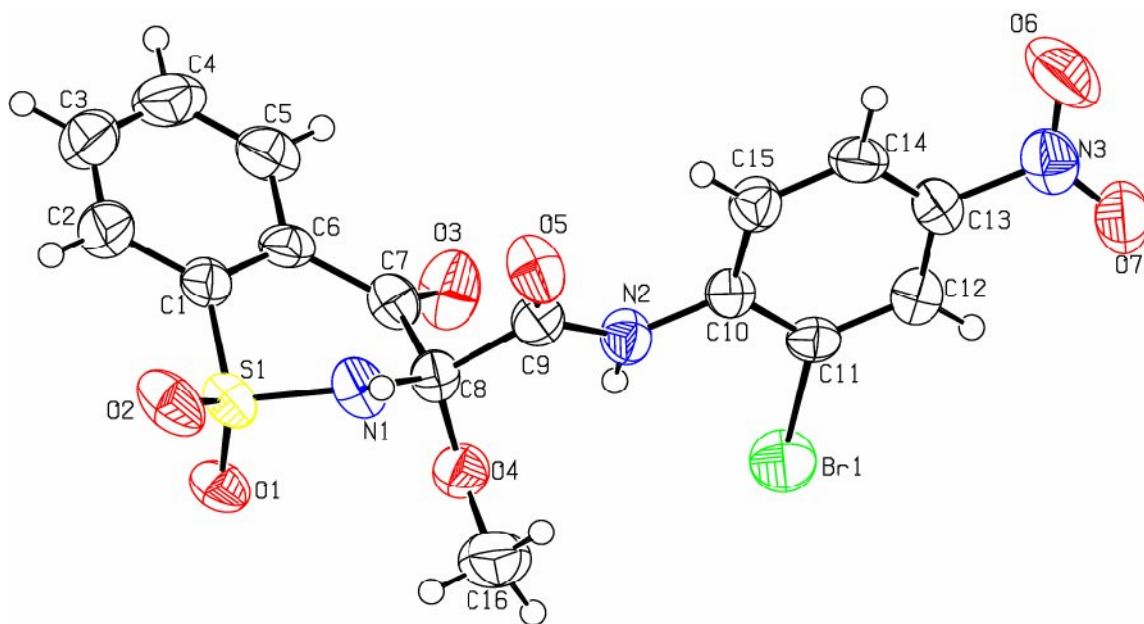


Fig. 1: ORTEP diagram of title compound, thermal ellipsoids were drawn at 50% probability level for non-hydrogen atoms.

#### Computational Methods

Density functional theory (DFT) investigations were performed by using Gaussian 09 software [35] in vacuo. Results/graphics were visualized by using GaussView 05 [36]. The energy minima structure was calculated by adopting B3LYP/6-31G (d, p) method. Frequency simulation was performed to confirm the true optimization. Simulated vibration was extracted from frequency output files. The  $^1\text{H-NMR}$  chemical shifts were calculated with the help of B3LYP/6-31G(d, p) method. The coefficients of frontier orbitals, molecular electrostatic potential (MEP) and reactivity indices were also calculated by adopting B3LYP/6-31G (d, p) method. The Mulliken and natural population (NBO) charges were calculated at the same level as used for optimization.

#### Results and Discussion

The benzothiazine derivative was synthesized as white crystalline solid in 86% yields, (for synthetic details see experimental section, Scheme-1). The crystallization of the molecule in methanol at room temperature yielded unsymmetrical ether with cyclic sultam and carboxamide functionality. Spectroscopic techniques like  $^1\text{H-NMR}$ , and IR were carried out initially to characterized molecule and then X-ray structural analysis proved the final structure.

#### Crystal Structure

The title benzothiazine derivative, having molecular formula  $[\text{C}_{16}\text{H}_{12}\text{N}_3\text{O}_7\text{SBr}]$  crystallized in

orthorhombic crystal system with  $Pbca2$  space group and  $Z = 8$ . The ORTEP plot benzothiazine derivative is shown in Fig. 1.

In the thiazine ring C8-carbon atom is chiral carbon with *R* configuration and adopted distorted tetrahedral geometry since the angles around it varies from  $104.1(3)^\circ$  to  $114.3(3)^\circ$ . Similarly, the sulfur atom (S1) also adopted tetrahedral type geometry having O1-S1-O2 angle of  $119.98(2)^\circ$ . The ring is stabilized by adopting like half-chair conformation along with N1 and S1 located away by  $0.3447(2)\text{\AA}$  and  $-0.3519(2)\text{\AA}$  from the plane of connected atoms C(1)/C(2)/C(7)/C(8)/N(1)/S(1). The root mean square (r. m. s.) deviation values for the thiazine ring is  $0.2300(2)\text{\AA}$ , which also indicates its non-planer behavior. The fused aromatic and thiazine rings are twisted at dihedral angles of  $14.43(1)^\circ$ . 2-Bromo-4-nitrophenyl ring is oriented at dihedral angles of  $70.83(5)^\circ$  and  $83.70(4)^\circ$  with respect to the planes produced by the fitted atoms of aromatic (C1-C6) and thiazine rings. The nitro group is twisted by  $15.29(5)^\circ$  with respect to its adjacent aromatic ring. The puckering parameters [37] are  $Q = 0.564(3)\text{\AA}$ ,  $\theta = 66.1(4)^\circ$ ,  $\varphi = 22.9(5)^\circ$ ,  $Q_{(2)} = 0.517(4)\text{\AA}$ ,  $Q_{(3)} = 0.228(4)\text{\AA}$  and  $\varphi_{(2)} = 22.9(5)^\circ$ .

The unit cell view is shown in Fig. 2 and the non-covalent interactions parameters are given in Table-1. Unit cell diagram is clearly depicting that the molecule exhibits  $\pi \cdots \pi$  interaction between the two aromatic rings (C10~C15 = Cg1) of neighboring molecules with

centroid distance = 3.755 Å and symmetry operation  $-x, -y, 2-z$ . Inter- and intra-molecular non-covalent interactions further facilitated to stabilize the crystal structure of molecule via classical and non-classical hydrogen bonding. Carboxamide N-H involve in N(2)-H...halogen (Br1) and N(2)-H...O(4) intramolecular interactions and form five membered ring motif  $S(5)$ . The intermolecular interactions of C(15)-H15...O2 and C(16)-H(16a)...O7 connected the molecules in zig-zag manner.

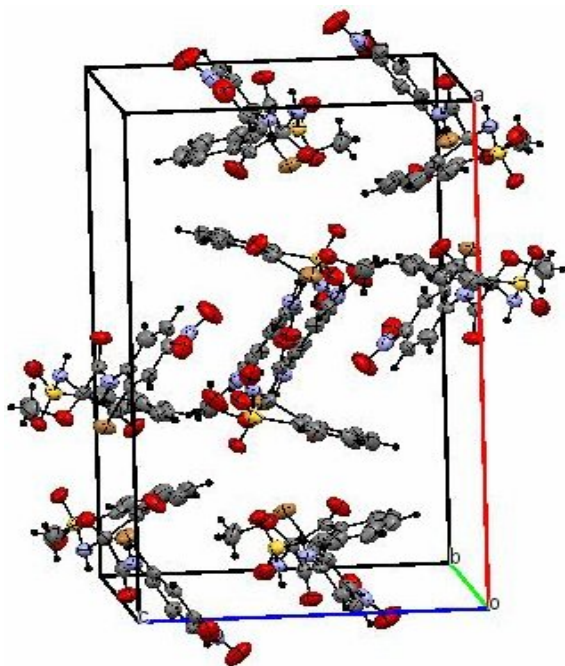


Fig. 2: Unit cell view, of Title compound.

Table-1: Hydrogen-bond Parameters of title Compound (Å, °) (Atomic Labels are with Reference to Fig. 1).

D-H...A(°)	d(D-A)(Å)	D(H...A)(Å)	d(D-H)(Å)	D-H...A
117.2	3.043(3)	2.55	0.86	N2-H2...Br1
112.9	2.653(5)	2.20	0.86	N2-H2...O4
149.7	3.202(5)	2.36	0.93	C15-H15...O2 <sup>1</sup>
120.7	2.976(5)	2.39	0.93	C15-H15...O5
159.4	3.459(6)	2.54	0.96	C16-H16A...O7 <sup>2</sup>

Symmetry Codes: <sup>1</sup>-X, 1-Y, 2-Z; <sup>2</sup>-X, -Y, 2-Z

Table-2: XRD and Computed Bond Lengths (Å) of Title Compound (Atomic Labels are with Reference to Fig. 1).

Bond length (B3LYP) (Å)	Bond length (XRD) (Å)	Bond	Bond length (B3LYP) (Å)	Bond length (XRD) (Å)	Bond
1.392	1.384(6)	C(1)-C(2)	1.910	1.879(4)	Br(1)-C(11)
1.406	1.394(6)	C(1)-C(6)	1.461	1.418(3)	S(1)-O(1)
1.395	1.365(7)	C(2)-C(3)	1.460	1.421(3)	S(1)-O(2)
1.397	1.386(7)	C(3)-C(4)	1.676	1.629(3)	S(1)-N(1)
1.391	1.383(6)	C(4)-C(5)	1.789	1.726(5)	S(1)-C(1)
1.403	1.395(6)	C(5)-C(6)	1.216	1.201(4)	O(3)-C(7)
1.489	1.479(6)	C(6)-C(7)	1.408	1.390(5)	O(4)-C(8)
1.569	1.545(6)	C(7)-C(8)	1.436	1.468(5)	O(4)-C(16)
1.568	1.564(6)	C(8)-C(9)	1.224	1.209(5)	O(5)-C(9)
1.412	1.403(5)	C(10)-C(11)	1.230	1.202(5)	O(6)-N(3)
1.407	1.388(6)	C(10)-C(15)	1.231	1.214(5)	O(7)-N(3)
1.385	1.374(5)	C(11)-C(12)	1.448	1.448(5)	N(1)-C(8)
1.392	1.376(6)	C(12)-C(13)	1.360	1.356(5)	N(2)-C(9)
1.391	1.374(5)	C(13)-C(14)	1.396	1.395(5)	N(2)-C(10)
1.388	1.372(6)	C(14)-C(15)	1.467	1.480(6)	N(3)-C(13)

### Geometry Optimization

In recent years, computational methods based on DFT have gained interest of scientists because of wide range applications. The DFT simulations of benzothiazine derivative were performed not only to theoretically simulate single crystal XRD results, but also to explore structural properties like frontier molecular orbital analysis (FMOs), chemical reactivity indices and molecular electrostatic potential (MEP). The Geometry of benzothiazine derivative was optimized by using 6-31G (d, p) basis set at DFT level, and shown in Fig. 3.

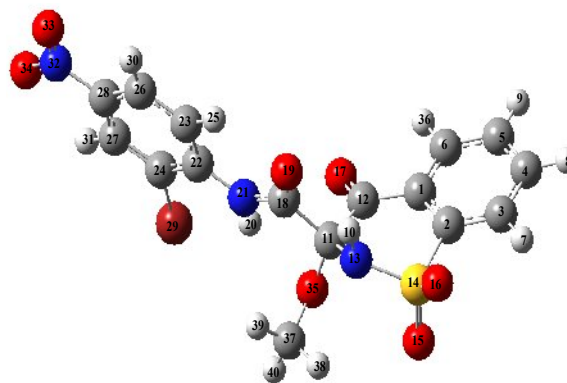


Fig. 3: Optimized geometry at B3LYP/6-31G (d, p) method.

A comparative analysis of XRD and computed bond lengths and bond angles is narrated in Table-2 and 3. From the data given in tables, it is clear that excellent correlation lies between XRD and simulated bond lengths and bond angles. Maximum deviation in the bond lengths is found in the range of 0.0 ~ 0.063 Å. Maximum deviation in bond length observed in S1-C1 (atomic labelling is in accordance with ORTEP plot Fig. 1) and for which the X-ray value is 1.726 Å and simulated value is equal to 1.789 Å. In bond angles, maximum deviation in X-ray and simulated data observed in the range of 0.01 ~ 3.53°. Maximum deviation is equal to 3.53° for C8-N1-S1.

Table-3: XRD and Simulated Bond Angles (°) of Title Compound.

Bond angle (B3LYP) (°)	Bond angle (XRD) (°)	Bond	Bond angle (B3LYP) (°)	Bond angle (XRD) (°)	Bond
117.83	118.8(4)	O(3)-C(7)-C(8)	121.51	119.98(19)	O(1)-S(1)-O(2)
120.41	119.6(4)	C(6)-C(7)-C(8)	106.41	107.83(18)	O(1)-S(1)-N(1)
114.70	115.0(4)	O(4)-C(8)-N(1)	109.13	107.94(19)	O(1)-S(1)-C(1)
102.84	104.1(3)	O(4)-C(8)-C(7)	107.93	107.24(19)	O(2)-S(1)-N(1)
111.68	111.8(3)	O(4)-C(8)-C(9)	108.20	110.8(2)	O(2)-S(1)-C(1)
115.50	114.3(3)	N(1)-C(8)-C(7)	101.86	101.46(19)	N(1)-S(1)-C(1)
104.67	105.4(3)	N(1)-C(8)-C(9)	116.21	114.9(4)	C(8)-O(4)-C(16)
107.40	106.1(4)	C(7)-C(8)-C(9)	120.33	116.8(3)	C(8)-N(1)-S(1)
126.96	127.3(4)	O(5)-C(9)-N(2)	128.53	129.9(4)	C(9)-N(2)-C(10)
120.76	122.8(4)	O(5)-C(9)-C(8)	124.85	125.2(5)	O(6)-N(3)-O(7)
112.26	109.9(4)	N(2)-C(9)-C(8)	117.50	117.6(5)	O(6)-N(3)-C(13)
118.95	118.6(4)	N(2)-C(10)-C(11)	117.64	117.2(5)	O(7)-N(3)-C(13)
122.71	122.3(4)	C(15)-C(10)-N(2)	118.78	121.7(4)	C(2)-C(1)-S(1)
118.33	119.1(4)	C(15)-C(10)-C(11)	121.47	120.9(5)	C(2)-C(1)-C(6)
120.18	120.2(3)	C(10)-C(11)-Br(1)	119.68	117.2(3)	C(6)-C(1)-S(1)
118.38	119.6(3)	C(12)-C(11)-Br(1)	119.18	119.0(5)	C(3)-C(2)-C(1)
121.43	120.2(4)	C(12)-C(11)-C(10)	120.27	122.0(5)	C(2)-C(3)-C(4)
118.58	119.1(4)	C(11)-C(12)-C(13)	120.18	118.7(5)	C(5)-C(4)-C(3)
118.76	118.3(4)	C(12)-C(13)-N(3)	120.53	120.8(5)	C(4)-C(5)-C(6)
119.60	119.9(5)	C(14)-C(13)-N(3)	118.34	118.6(4)	C(1)-C(6)-C(5)
121.63	121.8(4)	C(14)-C(13)-C(12)	123.89	122.6(4)	C(1)-C(6)-C(7)
119.40	119.3(4)	C(15)-C(14)-C(13)	117.74	118.8(5)	C(5)-C(6)-C(7)
120.61	120.5(4)	C(14)-C(15)-C(10)	121.73	121.6(4)	O(3)-C(7)-C(6)

Table-4: Prominent experimental and simulated vibrational (cm<sup>-1</sup>) frequencies of Title compound.

(Calc.)	(Exp.)	Assignment	(Calc.)	(Exp.)	Assignment	(Calc.)	(Exp.)	Assignment
3369	3350	$\nu_s$ N-H	1350	1322	$\nu_s$ S=O, $\beta$ N-H	1213	---	$\beta$ C-H <sub>arom.</sub>
1712	1750	$\nu_s$ C=O	1340	---	$\nu_s$ C-N	1187	1176	$\nu_s$ N-C
1601	---	$\nu_s$ C=C <sub>arom.</sub>	1312	---	$\nu_{as}$ C=C	1100	---	$\nu_s$ C-C, C-N
1578	1699	$\nu_s$ C=C <sub>arom.</sub>	1283	---	$\nu_{as}$ S=O	1094	---	$\nu_s$ N-C
1557	---	$\nu_s$ N=O, $\beta$ N-H	1261	---	$\beta$ C-H <sub>arom.</sub>	871	---	$\tilde{\alpha}$ C-H <sub>arom.</sub>
1520	---	$\nu_s$ C-N, $\nu_s$ C=C <sub>arom.</sub>	1251	---	$\beta$ C-H <sub>arom.</sub>	607	---	$\tilde{\alpha}$ N-H

$\nu_s$ , Symmetric stretching;  $\nu_{as}$ , Asymmetric stretching;  $\beta$ , In plane bending.

### Vibrational Analysis

The prominent experimental and theoretical vibration values are given in Table-4. Theoretical values always appear higher than experimental values, scaling factor (0.9627) was used to minimize the theoretical error. During comparison of main functional groups of title compound, stretching frequency of N-H appeared at 3350 cm<sup>-1</sup> in experimental spectrum. Whereas theoretically stretching vibration of NH appeared at 3369 cm<sup>-1</sup> and correlated with experimental value. For C=O experimental stretching vibration depicted at 1750 cm<sup>-1</sup> and comparatively simulated scan vibration appeared at 1712 cm<sup>-1</sup>. Results of experimental characterization showed strong stretching vibration of 1699 cm<sup>-1</sup>, assigned to aromatic C=C stretching, and on other hand theoretically same vibration is appeared at 1578 cm<sup>-1</sup>. In amide group, asymmetric stretching vibration assigned to C-N and it was in good correlation with theoretical peak at 1176 cm<sup>-1</sup>. In addition to stretching vibrations, some prominent vibrations are also observed in theoretical spectrum, which are difficult to assign in experimental scan. All these experimental and theoretical values were in good agreement with each other and confirmed the desired structure.

### <sup>1</sup>H-NMR studies

In order to validate the experimental NMR results, the experimental <sup>1</sup>H-NMR data is compared

with theoretically calculated <sup>1</sup>H-NMR which is measured in gas phase at B3LYP/6-31g (d, p) method and by using GIAO method. Tetramethylsilane is used as internal reference for which ppm is preferred. The comparative analysis of experimental and theoretical shift values is given in Table-5. In the title compound only amide, aromatic and methoxy protons are present. In experimental spectrum the NHCO proton is 8.55 ppm and theoretically the same proton is appeared at 9.71 ppm. The amide protons are always medium dependent, therefore are very difficult to compare both experimentally as well as theoretically. The benzene protons are appeared in the range of 7.64-8.42 ppm in experimental spectrum and during simulation in gaseous phase these are found in range of 7.82-9.23 ppm, respectively and correlated with the experimental values. In Experimental observation methoxy protons show peak at 3.68 ppm whereas theoretical simulation show peak at 3.79 ppm and corroborated nicely to each other.

Table-5: Comparison of experimental and simulated <sup>1</sup>H-NMR chemical shifts (ppm) (atomic labeling is in accordance with Fig. 3).

Proton	Exp. (CDCl <sub>3</sub> )	Calc. (Gas)
H <sub>20</sub> (CONH)	8.55	9.71
H <sub>7</sub> (aromatic)	7.64-8.42	8.0133
H <sub>8</sub> (aromatic)		7.9296
H <sub>9</sub> (aromatic)		7.8288
H <sub>25</sub> (aromatic)		9.2386
H <sub>30</sub> (aromatic)		8.4202
H <sub>31</sub> (aromatic)		8.6185
H <sub>36</sub> (aromatic)		8.4264
H <sub>38-40</sub> (OCH <sub>3</sub> )	3.68	3.79

### Frontier Molecular Orbital (FMOs) Analysis and Electronic Properties

Frontier molecular orbitals (FMOs) analysis by DFT methods has proved very useful to explore electronic and absorption properties of molecules [38]. In molecular interactions mainly, frontier orbitals (HOMO/LUMO) participate. The HOMO-LUMO surfaces are shown in the Fig. 4 along with corresponding energies of HOMO, LUMO and HOMO-LUMO band gap.

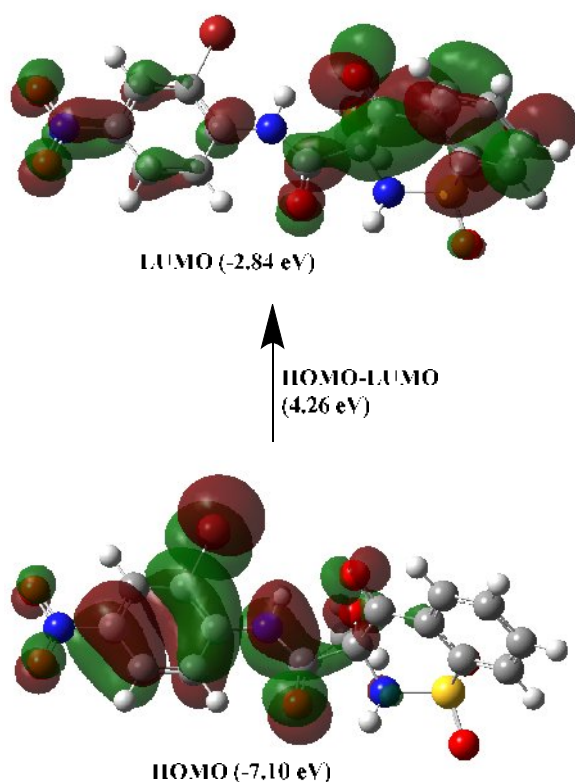


Fig. 4: HOMO and LUMO Surfaces along corresponding energies.

The FMO analysis revealed that compound has total 118 occupied orbitals, HOMO is concentrated on nitro and bromo substituted phenyl ring and amide functionality, whereas LUMO are mainly concentrated on the benzothiazine moiety. Energy of HOMO (I. P) and LUMO (E. A) were observed -7.10 eV and -2.84 eV. The HOMO-LUMO band gap found equal to 4.26 eV, which indicates, that compound is kinetically less stable and more reactive.

### Reactivity Indices

DFT can also be used to describe the chemical reactivity of any organic compound in term of chemical hardness ( $\eta$ ), electrophilicity index ( $\omega$ )

and electronic chemical potential ( $\mu$ ) [24]. The chemical hardness ( $\eta$ ) of a compound is defined by the mathematical expression given below (1).

$$\eta = (E_{\text{HOMO}} - E_{\text{LUMO}})/2 \quad (1)$$

Electronic chemical potential ( $\mu$ ) is a negative of electronegativity [30] and mathematically, can be expressed by equation (2).

$$\mu = (E_{\text{HOMO}} + E_{\text{LUMO}})/2 \quad (2)$$

Electrophilicity index ( $\omega$ ) is a thermodynamics property and plays a key role in explaining the reactivity of any system and can be expressed by mathematical relation given below (3) [24].

$$\omega = \mu^2/2\eta \quad (3)$$

Using the above mathematical equations (1-3) the three reactivity indices of benzothiazine derivatives were calculated and the data is listed in Table-6, along with optimized energy and dipole moment. The chemical hardness of title compound is 2.128 eV, which reflects that compound is chemically less hard and more reactive. Similarly the high electrophilicity index value i.e. 5.813 eV is reflecting title compound is more nucleophilic in nature. The electronic chemical potential value is 4.974 eV, again is indicative of high reactivity of title compound.

Table-6: Reactivity indices like chemical hardness ( $\eta$ ), electrophilicity index ( $\omega$ ), electronic chemical potential ( $\mu$ ) of Title Compound

Calculated Values	Properties
-4277.4989072	Electronic energy (hf)
-7.10	$E_{\text{HOMO}}$ (eV)
-2.84	$E_{\text{LUMO}}$ (eV)
2.128	Chemical hardness (eV)
4.974	Electronic chemical potential (eV)
5.813	Electrophilicity index (eV)

### Molecular Electrostatic Potential (MEP)

Molecular electrostatic potential (MEP) mapping explains the nucleophilic and electrophilic regions in any compound, and proved as very important tool in quantum chemical chemistry. It describes the chemical behavior of a system by predicting electrophilic and nucleophilic sites on the basis of color code in a molecule [40]. MEP is a basic property, which explains the behavior of target molecule and demonstrates the relative polarity of a compound [41]. Mathematically, MEP can be defined by the relation given below.

$$V(r) = \sum \frac{Z_A}{|R_A - r|} - \int \frac{\rho(r')}{|r' - r|} dr'$$

MEP is very important in structural biology, to understand the monovalent interactions [42]. In MEP analysis, electrophilicity and nucleophilicity is explained on the basis of different color codes, red

color indicates nucleophilic and blue color reflects electrophilic site [43]. Molecular electrostatic potential surface of title benzothiazine derivative is shown in the (Fig. 5).

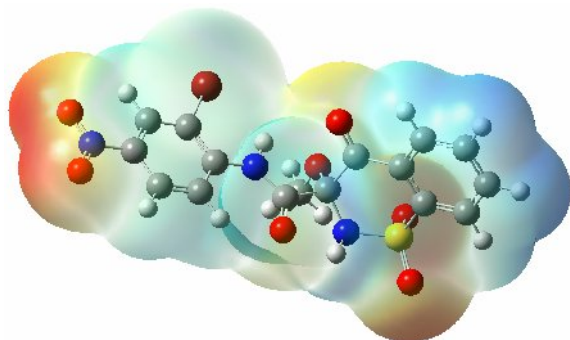


Fig. 5: MEP surface simulated at B3LYP/6-31G (d, p) method.

The MEP analysis of compound revealed that, the positive potential of the target molecule is found  $4.381 \times 10^{-3}$  a. u. and concentrated on the benzene ring of benzothiazine moiety. The negative potential of the target molecule found  $-4.381 \times 10^{-3}$  a. u and preferred site for electrophilic attack is nitro group attached to phenyl moiety.

#### Mulliken and Natural Population Analysis

One of the most effective applications of quantum chemical calculations is the simulation of effective atomic charges for molecular structure. Mulliken and natural population (NBO) analyses are the common methods to measure the atomic charges. Natural population charges can be measured with the help of NBO (natural bond analysis), whereas Mulliken population analysis is totally based on total atomic charges. The Mulliken and natural population charges are given in the Table-7.

The negative charge is obtained on N13 (-0.674, -0.954), O15 (-0.504, -0.922), O16 (-0.511, -0.93), and these atoms are directly attached to sulfur (1.223, 2.369) make it more positive. Methoxy oxygen attached to carbon (C11) has negative charge (-0.189, -0.24) and directly attached carbon is positively charged (C11, 0.294, 0.307). Oxygen (O17) atom attached to thiazine ring creates positive charge on C12 (0.409, 0.566) of ring due to its negative charge (-0.512, -0.519). Amide group in between benzene and thiazine moieties has consistency in results, N21 (-0.617, -0.630) and O19 (-0.609, -0.512) are negatively charged and transfer positive charge on C18 (0.594, 0.688) and H<sub>2</sub>O (0.311, 0.461). Nitro group (-0.403, -0.25) attached to benzene ring is electron

withdrawing group thus it causes electropositive charge on C28 (0.25, 0.053, Table-2). The intermolecular hydrogen bonding is observed between bromine of bromo substituted aromatic ring and the oxygen of methoxy group, and on the other hand methoxy group proton form intermolecular hydrogen bonding with oxygen of nitro group. Bromo substituted aromatic ring having positively charged protons, they formed hydrogen bond with oxygen of sulfoxide and nitro groups of other molecules, as shown in the unit cell packing diagram (Fig. 2) (for detailed charges see the Table-7).

Table-7: Mulliken and natural population charges (NBO) of Title compound (tables are according to the Fig. 3).

Atom	Mulliken Charges	Natural population charges (NBO)
C1	0.082	-0.153
C2	-0.217	-0.286
C3	-0.093	-0.219
C4	-0.067	-0.195
C5	-0.083	-0.223
C6	-0.081	-0.168
H7	0.143	0.273
H8	0.117	0.256
H9	0.115	0.255
H10	0.321	0.465
C11	0.294	0.307
C12	0.409	0.566
N13	-0.674	-0.954
S14	1.223	2.369
O15	-0.504	-0.922
O16	-0.511	-0.930
O17	-0.447	-0.519
C18	0.594	0.688
O19	-0.512	-0.609
H20	0.311	0.461
N21	-0.630	-0.617
C22	0.342	0.166
C23	-0.100	-0.244
C24	0.007	-0.129
H25	0.158	0.287
C26	-0.105	-0.202
C27	-0.103	-0.22
C28	0.254	0.053
Br29	-0.078	0.091
H30	0.148	0.281
H31	0.159	0.293
N32	0.387	0.513
O33	-0.394	-0.380
O34	-0.396	-0.383
O35	-0.496	-0.576
H36	0.136	0.270
C37	-0.082	-0.334
H38	0.155	0.235
H39	0.102	0.201
H40	0.132	0.234

#### Conclusion

In conclusion, title benzothiazine derivative was synthesized in respectable yields, final structure is confirmed with the help of single crystal XRD analysis along-with vibrational and magnetic spectroscopic techniques. Theoretical investigations were accomplished and the results were compared with the experimental findings, which showed a good agreement between these (experimental and theoretical values). X-ray crystal structures with

orthorhombic crystal system, *Pbca* space group,  $a = 20.813(1)$ ,  $b = 13.187(7)$ ,  $c = 13.062(8)$  Å,  $\alpha = \beta = \gamma = 90^\circ$ ,  $V = 3584.8(3)$  Å<sup>3</sup>,  $Z = 8$  and  $D_c = 1.743$  g·cm<sup>-3</sup> was found in good relation with simulated structural results with minor difference in bond lengths and bond angles. Theoretical and simulated spectroscopic (1H-NMR and FT-IR) results corroborated to each other, very nicely. The coefficients of HOMO and LUMO were simulated for the first time and HOMO-LUMO energy gap showed 4.25 eV, which is showing that compound, is highly reactive in nature. Reactivity indices and molecular electrostatic potential were simulated to investigate the structural properties. Mulliken and natural population charges analyses confirmed intra and intermolecular hydrogen bonding.

#### Acknowledgements

The authors are highly thankful to Higher Education Commission Pakistan (HEC) for financial support (Grant no. 20-3013/NRPU/R&D/HEC/14/525). The authors acknowledge COMSATS Institute of Information Technology Abbottabad for financial support as well.

#### References

- M. N. Arshad, W. A. Siddiqui, I. U. Khan and A. M. Asiri, Ligand Free Pd Catalyzed Cyclization-Influence of Steric Hindrance, *J. Chil. Chem. Soc.*, **59**, 2697 (2015).
- R. Banerjee, H. Chakraborty and M. Sarkar, Photophysical Studies of Oxycam Group of NSAIDs: Piroxicam, Meloxicam and Tenoxicam, *Spectrochim Acta. A: Mol. Biomol. Spectrosc.*, **59**, 1213 (2003).
- M. Shafiq, M. Zia-Ur-Rehman, I. U. Khan, M. N. Arshad and S. A. Khan, Synthesis of Novel Anti-Bacterial 2,1-benzothiazine 2,2-dioxides derived from methyl anthranilate, *J. Chil. Chem. Soc.*, **56**, 527 (2011).
- N. I. Ahmad, M. Zia-ur-Rehman, H. L. Siddiqui, M. F. Ullah, M. Parvez, Microwave Assisted Synthesis and Structure-Activity Relationship of 4-hydroxy-N'-[1-phenylethylidene]-2H/2-methyl-1,2-benzothiazine-3-carbohydrazide 1,1-dioxides as Anti-Microbial Agents, *Eur. J. Med. Chem.*, **46**, 2368 (2011).
- M. Shafiq, I. U. Khan, M. Zia-ur-Rehman, M. N. Asghar, A. M. Asiri and M. N. Arshad, Synthesis and Antioxidant Activity of New Series of 2,1-benzothiazine-2,2-dioxide Hydrazine Derivatives, *Asian J. Chem.*, **24**, 4799 (2012).
- M. R. Gannarapu, S. B. Vasamsetti, N. Punna, N. K. Royya, S. R. Pamulaparthi, J. B. Nanubolu, S. Kotamraju, N. Banda, Synthesis of novel 1,2-benzothiazine 1,1-dioxide-3-ethanone oxime N-aryl Acetamide Ether Derivatives as Potent Anti-Inflammatory Agents and Inhibitors of Monocyte-to-Macrophage Transformation, *Eur. J. Med. Chem.*, **8**, 143 (2014).
- W. Jie, X. Qinlong and L. Jiaming, Design, Synthesis and Biological Activity of 1,2-Benzothiazine Derivatives as Potential Anticancer Agents, *Chin. J. Org. Chem.*, **34**, 2040 (2014).
- J. G. Lombardino, Synthetic Method and Intermediate of Piroxicam, U. S. Patent-19811013 (1981).
- J. G. Lombardino, Isomeric 3,4-dihydro-2H-1,2-benzothiazine 1,1-dioxides valuable for their Chemotherapeutic Qualities, U. S. Patent-3591584 (1971).
- R. A. Abramovitch, K. M. More, I. Shinkai, P. C. Srinivasan, Ring-Expansion of 3-bromoalkyl-1,2-benzisothiazole 1,1-dioxides to (2H)-1,2-benzothiazin-4(3H)-one 1,1-dioxides, *J. Chem. Soc. Chem. Commun.*, **19**, 771 (1976).
- H. Zinnes, N. A. Lindo, J. C. Sircar, M. L. Schwartz, J. J. Shavel, 1,2-Benzothiazines. 6. 3-Carbamoyl-4-hydroxy-2H-1,2-benzothiazine 1,1-dioxides as antiinflammatory agents, *J. Med. Chem.*, **16**, 44 (1973).
- J. G. Lombardino, Benzothiazinecarboxamide dioxides, U. S. Patent-3957772 (1976).
- J. G. Lombardino, H. A. J. Watson, New Synthetic Approaches to 3-carboxamides of 4-hydroxy-2H-1,2-benzothiazine 1,1-dioxide., *J. Heterocycl. Chem.*, **13**, 333 (1976).
- W. A. Siddiqui, S. Ahmad, I.U. Khan, H. L. Siddiqui and G. W. Weaver, Facile One-Pot Synthesis of 4-Hydroxy-2-methyl-(2H)-1,2-benzothiazine-3-sulfonic Acid 1,1-Dioxide, *Synthic. Commun.*, **37**, 767 (2007).
- S. Parveen, S. Hussain, X. Qin, X. Hao, S. Zhu, M. Rui, S. Zhang, F. Fu, B. Ma, Q. Yu, C. Zhu, Copper-Catalyzed Asymmetric Synthesis and Comparative Aldose Reductase Inhibition Activity of (+)/(-)-1,2-Benzothiazine-1,1-dioxide Acetic Acid Derivatives, *J. Org. Chem.*, **79**, 4963 (2014).
- M. Zia-ur-Rehman, J. A. Choudhary and S. Ahmad, An Efficient Synthesis of 2-Alkyl-4-hydroxy-2H-1,2-benzothiazine-3-carboxamide-1,1-dioxides, *Bull. Korean Chem. Soc.*, **26**, 1771 (2005).
- A. Cartier, N. C. Thomson, P. A. Frith, R. Roberts, F. E. Hargreave, Allergen-Induced Increase in Bronchial Responsiveness to Histamine: Relationship to the Late Asthmatic



- Response and Change in Airway Caliber, *J. Allergy Clin. Immunol.*, **70**, 170 (1982).
18. P. Durrington, Dyslipidaemia, *The Lancet.*, **362**, 717 (2003).
  19. G. Y. Shvarts, New Trends in the Creation of Anti-Inflammatory Drugs (a review), *Pharm. Chem. J.*, **22**, 827 (1988).
  20. I. Villegas, M. J. Martin, C. C. La, V. Motilva, L. C. De La, A. Effects of Oxicam Inhibitors of Cyclooxygenase on Oxidative Stress Generation in Rat Gastric Mucosa. A Comparative Study, *Free Radical Res.*, **36**, 769 (2002).
  21. T. U. Rahman, M. Arfan, T. Mahmood, W. Liaqat, M. A. Gilani, G. Uddin, R. Ludwig, K. Zaman, M. I. Choudhary, K. F. Khattak and K. Ayub, Isolation, Spectroscopic and Density Functional Theory Studies of 7-(4-methoxyphenyl)-9H-furo[2,3-f]chromen-9-one: A New Flavonoid from the Bark of *Milletia ovalifolia*, *Spectrochim. Acta. A: Mol. Biomol. Spectrosc.*, **146**, 24 (2015).
  22. F. Aman, A. M. Asiri, W. A. Siddiqui, M. N. Arshad, A. Ashraf, N. S. Zakharov and V. A. Blatov, Multilevel Topological Description of Molecular Packings in 1, 2-benzothiazines, *CrystEngComm.*, **16**, 1963 (2014).
  23. M. N. Arshad, A. M. Asiri, K. A. Alamry, T. Mahmood, M. A. Gilani, K. Ayub and A. S. Birinji, Synthesis, Crystal Structure, Spectroscopic and Density Functional Theory (DFT) Study of *N*-[3-anthracen-9-yl-1-(4-bromophenyl)-allylidene]-*N*-benzenesulfonylhydrazine, *Spectrochim. Acta. A: Mol. Biomol. Spectrosc.*, **142**, 364 (2015).
  24. M. N. Arshad, A. Bibi, T. Mahmood, A. M. Asiri and K. Ayub, Synthesis, Crystal Structures and Spectroscopic Properties of Triazine-Based Hydrazone Derivatives; a Comparative Experimental-Theoretical Study, *Molecules.*, **20**, 5851 (2015).
  25. M. N. Arshad, T. Mahmood, A. F. Khan, M. Zia-Ur-Rehman, A. M. Asiri, I. U. Khan, R. Un-Nisa, K. Ayub, A. Mukhtar and M. T. Saeed, Synthesis, Crystal Structure and Spectroscopic Properties of 1,2-benzothiazine derivatives: An Experimental and DFT Study, *Chin. J. Struct. Chem.*, **34**, 15 (2015).
  26. L. A. Taib, H. M. Faidallah, Z. S. Şahin, A. M. Asiri, O. Şahin, M. N. Arshad, Synthesis, Spectral Analysis, X-Ray Crystal Structures and Evaluation of Chemical Reactivity of Five New Benzoindazole Derivatives Through Experimental and Theoretical Studies, *J. Mol. Struct.*, **1076**, 272 (2014).
  27. O. A. Blatova, A. M. Asiri, Z. M. Al-amshany, M. N. Arshad, V. A. Blatov, Molecular Packings and Specific-Bonding Patterns in Sulfonamides, *New J. Chem.*, **38**, 4099 (2014).
  28. M. N. Arshad, O. Sahin, M. Zia-ur-Rehman, I. U. Khan, A. M. Asiri, H. M. Rafique, 4-hydroxy-2H-1, 2-benzothiazine-3-carbohydrazide 1, 1-dioxide-oxalohydrazide (1:1): X-Ray Structure and DFT Calculations, *J. Struct. Chem.*, **54**, 437 (2013).
  29. Agilent, CrysAlis PRO (2012). Agilent Technologies, Yarnton, England.
  30. G. M. Sheldrick, A Short History of SHELX, *Acta Cryst. A.*, **64**, 112 (2008).
  31. L. J. Farrugia, ORTEP-3 for Windows, *J. Appl. Crystallog.*, **30**, 565 (1997).
  32. A. L. Spek, PLATON-A Multipurpose Crystallographic Tool. Utrecht, Utrecht University, The Netherlands, (2005).
  33. L. J. Farrugia, WINGX-A Windows Program for Crystal Structure Analysis, University of Glasgow, 1998.
  34. L. J. Farrugia, WinGX Suite for Small-Molecule Single-Crystal Crystallography, *J. Appl. Crystallogr.*, **30**, 837 (1999).
  35. M. J. Frisch, G. W. Trucks, H. B. Schlegel, G. E. Scuseria, M. A. Robb, J. R. Cheeseman, G. Scalmani, V. Barone, B. Mennucci, G. A. Petersson, H. Nakatsuji, M. Caricato, X. Li, H. P. Hratchian, A. F. Izmaylov, J. Bloino, G. Zheng; J. L. Sonnenberg, M. Hada, M. Ehara, K. Toyota, R. Fukuda, J. Hasegawa, M. Ishida, T. Nakajima, Y. Honda, O. Kitao, H. Nakai, T. Vreven, J. A. Jr. Montgomery, J. E. Peralta, F. Ogliaro, M. Bearpark, J. J. Heyd, E. Brothers, K. N. Kudin, V. N. Staroverov, R. Kobayashi, J. Normand, K. Raghavachari, A. Rendell, J. C. Burant, S. S. Iyengar, J. Tomasi, M. Cossi, N. Rega, J. M. Millam, M. Klene, J. E. Knox, J. B. Cross, V. Bakken, C. Adamo, J. Jaramillo, R. Gomperts, R. E. Stratmann, O. Yazyev, A. J. Austin, R. Cammi, C. Pomelli, J. W. Ochterski, R. L. Martin, K. Morokuma, V. G. Zakrzewski, G. A. Voth, P. Salvador, J. J. Dannenberg, S. Dapprich, A. D. Daniels, Ö. Farkas, J. B. Foresman, J. V. Ortiz, J. Cioslowski, Fox. D. J. Gaussian, Inc., Wallingford CT (2010). Gaussian 09, Revision C.01.
  36. D. Roy, K. Todd, M. John, Semichem, Inc., Shawnee Mission, KS, (2009). GaussView, Version 5.
  37. D. Cremer and J. A. Pople, General Definition of Ring Puckering Coordinates, *J. Am. Chem. Soc.*, **97**, 1354 (1975).
  38. H. Ullah, A. Rauf, Z. Ullah, Fazl-i-Sattar, M. Anwar, A. H. A. Shah, G. Uddin, K. Ayub, Density Functional Theory and Phytochemical

- Study of Pistagremic acid, *Spectrochim. Acta*, **118A**, 210 (2014).
39. S. S. Halilovic, M. Salihovic, H. D. Cancar, S. Trifunovic, S. Roca, D. Softic, D. Završnik, DFT Study and Microbiology of Some Coumarin-Based Compounds Containing a Chalcone Moiety, *J. Serb. Chem. Soc.*, **79**, 435 (2014).
  40. L. Szabo, V. Chiş, A. Pirnau, N. Leopold, O. Cozar and S. Orosz, Spectroscopic and Theoretical Study of Amlodipine Besylate, *J. Mol. Struct.*, **924**, 385 (2009).
  41. M. Bartoskova and Z. Friedl, The Relationship between the Heats of Formation and the Molecular Electrostatic Potentials of Polyazaarenes, *Cent. Eur. J. Energ. Mat.*, **10**, 103 (2013).
  42. E. Scrocco and J. Tomasi, Electronic Molecular Structure, Reactivity and Intermolecular Forces: An Euristic Interpretation by Means of Electrostatic Molecular Potentials, *Adv. Quantum Chem.*, **11**, 115 (1978).
  43. F. J. Luque, J. M. Lopez, M. Orozco, Perspective on "Electrostatic Interactions of a Solute with a Continuum. A Direct Utilization of an Initial Molecular Potentials for the Prediction of Solvent Effects, *Theor. Chem. Acc.*, **103**, 343 (2000).